European Review for Medical and Pharmacological Sciences 2015; 19: 835-843

Radioactive iodine labeling of monoclonal antibody against Hsp90α and its use in diagnostic imaging in prostate cancer xenograft model

H.-W. SUN, R.-F. WANG, P. YAN, C.-L. ZHANG, P. HAO, H. MA, X.-Q. CHEN

Department of Nuclear Medicine, Peking University First Hospital, Beijing, China

Abstract. – OBJECTIVE: Heat shock protein (Hsp90) resides exclusively in the cytosol in normal cells, but is activated and then removes to the cell surface in tumor cells. The detecting up-regulation or activation of Hsp90 is an early indicator of malignant behavior of cancer cells. Hsp90 has emerged as an important target for diagnosis or therapy of prostate cancer. In this study, we labeled Hsp90α specific monoclonal antibody (Hsp90α-mAb) with radioiodine Na^{131}I and investigated its potential usage in diagnostic imaging of prostate tumor in xenograft mice model.

METHODS: Hsp90α-mAb was radioiodinated by using chloramine-T. The radiolabeling efficiency and radiochemical purity were assessed in vitro. ^{131}I-Hsp90α-mAb was then injected into the nude mice bearing human prostate carcinoma. The planar gamma Imaging was performed at 3, 6, 9 and 12 h after injection.

RESULTS: The radiochemical purity of ^{131}I-Hsp90α-mAb exceeded 95% after purification. This radiolabeled mAb was stable in human blood serum. In planar gamma imaging study, the prostate tumors in mice model were imaged clearly at 3h after injection of ^{131}I-Hsp90α-mAb.

CONCLUSIONS: The results suggest that ^{131}I-HSP90α-mAb could be a new promising molecular probe for diagnostic imaging of prostate tumors.

Key Words:
Hsp90α, Monoclonal antibody, Molecular imaging, ^{131}I, Radiolabel.

Introduction

Heat shock proteins (Hsp) were initially found in 1962, whose abundance increases upon heat stress[1]. These proteins play an essential role in many cellular processes such as cell cycle control, cell survival, hormone and other signaling pathways[2,3]. Heat shock protein 90 (Hsp90) is a highly conserved molecular chaperone and essential for viability of eukaryotic cells. A large number of proteins have been found to be Hsp90-dependent client proteins including more than two-thirds of protein kinases, many transcription factors, and E3-ligases et al[4]. Most of these client proteins will be directed to proteasomal degradation when Hsp90 fails its task[5]. Hsp90 usually functions to maintain the structural and functional integrity of its client proteins. Some of the established Hsp90 clients play a central role in human diseases including cancer, neurodegenerative disorders and viral infections. Recently, several key oncogenic proteins have been found to be Hsp90 clients that are involved in signal transduction pathways responsible for proliferation, cell cycle progression, apoptosis, angiogenesis, and metastasis of cancer cell[6-8].

Hsp90 has at least four distinct isoforms, i.e. the mostly inducible Hsp90α, the constitutively expressed Hsp90 , mitochondria isoform Trap1, and endoplasmic reticulum isoform Grp94[9,10]. All Hsp90 isoforms have the same domain architecture with an N-terminal nucleotide binding domain, a middle domain and a C-terminal dimerization site. Hsp90 is constitutively expressed at 2- to 10-fold higher levels in tumor cells compared to their normal counterparts. Mutated or overexpressed kinases like Akt[11], ErbB2/HER2[12], and Raf1[13] are closely associated with the overexpressed Hsp90 to control cancerogenic growth. Interestingly, while Hsp90 resides exclusively in the cytosol in normal cells, the overexpressed Hsp90 is activated and removes to the surface of cancer cells. Thus, Hsp90 has emerged as an important target in cancer therapy.

A number of researchers have reported the study of radioiodine in diagnosis or treatment of human cancers such as thyroid cancer[14-17]. In this

Corresponding Author: Rong-Fu Wang, MD; e-mail: rongfu_wang@163.com

study, we labeled Hsp90a specific monoclonal antibody (Hsp90a-mAb) with radioiodine $Na^{131}I$ and then tested its usage in diagnostic imaging of prostate cancer xenograft in mice model.

Methods

Radiolabeling

Radioiodination of Hsp90α-mAb was performed using the chloramines-T (CH-T) method. 10 μg of Hsp90α mAb were dissolved in 51 μl of phosphate buffer (PB, 0.05M, pH 7.4). 40 μl $Na^{131}I$ (74 MBq) was added to the solution. 9 μl CH-T (10 mg/ml) was then added to the reaction mixture. The reaction mixture was gently agitated for 5 min at 20 and then quenched by adding 45 μl sodium metabisulfite (4.0 mg/ml in 0.1 mol/L PB, pH 7.4). The radiolabeling yield was measured by performing a double-phase paper chromatography using Xinhua No. 1 filter paper and n-butanol:ethanol:ammonia water (5:1:2) as mobile phase. The conditions of reaction were optimized to increase labeling yields by changing the labeling time, reaction temperature and weight ratio of mAb to CH-T. The Hsp90a-mAb (ab59459) was purchased from Abcam Inc.

Purification and Radiochemical Purity Test

The radio-labeled Hsp90α-mAb was further purified by chromatography on a Sephadex G-25 column (1 × 20 cm) at 20°C. The bound proteins were first eluted with 1% bovine serum albumin and then eluted with phosphate-buffered saline (PBS, 0.1 M, pH 7.4). The eluted fractions were collected at an elution rate of 0.5 ml/min, 5 drops/fraction. The radiochemical purity was determined by a double-phase paper chromatography on Xinhua No.1 filter paper with n-butanol:ethanol:ammonia water (5:1:2) as mobile phase. The intensity of the radioactivity of all the fractions was detected using radioactivity meters (National Institute of Metrology, Beijing, China). The mAb content of all fractions was measured at 280 nm using an ND-1000 spectrophotometer (Nanodrop Technologies, Wilmington, DE, USA). Radiochemical purity of ^{131}I-Hsp90α-mAb were also analyzed by performing HPLC using an Shimadzu System with SCL-10AVP HPLC pump consisting of an Alltima C-18 column (250 mm´4.6 mm, 5 mm) with CH_3CN as a mobile phase at a flow rate of 1 ml/min. The purified ^{131}I-Hsp90α-mAb was put in human blood serum or saline at 37°C and the radiochemical purities were examined at 3, 6, 9, 12 and 24 h to determine the stability of labeled mAb.

Cell Culture

Human prostate cancer cell line DU145 was obtained as a generous gift from Institute of Urology, Peking University and used in this study. The cell line was maintained in Roswell Park Memorial Institute-1640 culture medium supplemented with 10% fetal bovine serum (FBS) and 100 mg/ml of penicillin-streptomycin (Gibco, Grand Island, NY, USA) under standard conditions (37°C, 5% CO_2).

Cellular Uptake Assay

In vitro cellular uptake of ^{131}I-Hsp90α-mAb was analyzed in 24-well plates with $1x10^5$ DU145 cells per well under two conditions: in the presence or absence of unlabeled Hsp90 -mAb. For control group, 10 g of unlabeled Hsp90α-mAb in 10 ml PBS were averagely added into each well half an hour before experiment. For both groups, 100 μCi of ^{131}I-Hsp90α-mAb in 10 ml of PBS were added averagely into each well. Cells were then incubated at 37°C and harvested at 1, 3, 6, 9, 12, and 24 hours. Each well was rinsed with PBS for 3 times. C_{out} was defined as the counts of radioactive medium and PBS. After rinsing, the cells were lysed in solution containing 0.5 M sodium hydroxide and 1% sodium dodecyl sulfate and the radioactivity counts were determined as C_{in}. Cellular uptake ratio was calculated by using the formula $C_{in}/(C_{in} + C_{out})$.

Animal Models

Single photon emission computed tomography (SPECT) imaging was carried out in 4 week-old male Nunu nude mice (Department of Laboratory Animal Science at Peking University, Beijing, China). To generate solid tumors, $5x10^6$ DU145 tumor cells were injected into the armpits of athymic nude mice and allowed to grow for 3 weeks until the tumors were about 1.0 cm^3 in size. This study was carried out in strict accordance with the recommendations in the Guide for the Care and Use of Laboratory Animals (Ministry of Science and Technology of China, 2006). Animal fear and pain were reduced to the lowest degree. This protocol has been approved by the committee of experimental animal ethics of the first Hospital of Peking University with the permit No. 201333.

SPECT and Micro-PET Imaging

Each group has six Nunu nude mice bearing human carcinoma. Three of them were injected with saline and other three with unlabeled Hsp90α-mAb 1h before experiment. Each mouse was then injected intravenously with 7.4 MBq of ^{131}I-Hsp90α-mAb. All the animals were imaged by SPECT with a single head rotating scintillation camera (MPR from General Electric Company, Fairfield, CT, USA) at 3, 6, 9 and 12 h post-injection. The camera is equipped with a high-energy general purpose collimator (HEGP). The acquisition count is 200000.

In micro-positron emission tomography (PET) group, the mice had been fasting for 10 h before ^{18}F-FDG injections but allowed free access to water. After being intraperitoneally anesthetized with pentobarbital (100 mg/kg, Sigma-Aldrich, Saint Louis, MO, USA), each mouse was injected intravenously with an approximate 3.7 MBq of ^{18}F-FDG. Micro-PET imaging and analysis were performed using a MOSAIC animal PET scanner (Philips Medical Systems, Andover, MA, USA) with attached software (version 9.4). A conventional imaging of 10 min duration was performed in the prone position at 1 h post-injection and a delayed imaging of 10 min was performed at 2 h. The maximum counts were recorded by drawing regions of interest (ROI) over the tumor and the homo-lateral muscle on the coronal images, respectively. Tumor-to-muscle (T/M) ratio was compared by the maximum counts.

Statistical Analysis

ANOVA analysis was performed to statistically analyze the data. The results are presented as mean values ± standard deviation (SD). p values < 0.05 were considered statistically significant.

Results

Hsp90α-mAb Was Stably Radioiodinated with High Radiochemical Purity

In this study, Hsp90α-mAb was successfully radiolabeled with ^{131}I under optimal conditions. The labeling efficiency and radiochemical purity of ^{131}I-Hsp90α-mAb were determined by performing paper chromatography. ^{131}I-Hsp90α-mAb showed an R_f value of nearly 0.1 whereas the R_f of free ^{131}I was between 0.9-1.0. We observed that the labeling efficiency approaches the maximum when Hsp90α-mAb/chloramine-T weight ratio is 0.6:1 (Figure 1A) and the reaction is incubated at 20°C (Figure 1B) for 5 min (Figure 1C).

^{131}I-Hsp90α-mAb was purified by chromatography on a Sephadex G-25 column. Figure 2 shows

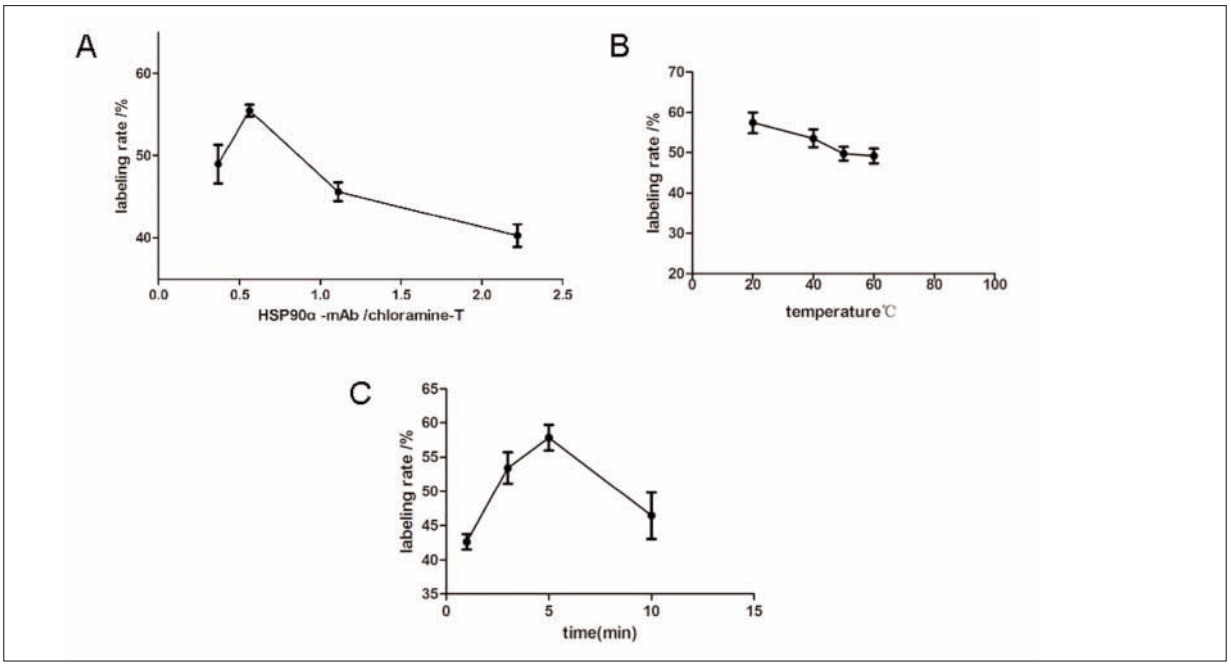

Figure 1. Labeling of Hsp90α-mAb with ^{131}I. Shown is the relationship between radiolabeling yields and Hsp90α-mAb/CH-T weight ratio ***(A)***, reaction temperature ***(B)***, or time period of incubation ***(C)***.

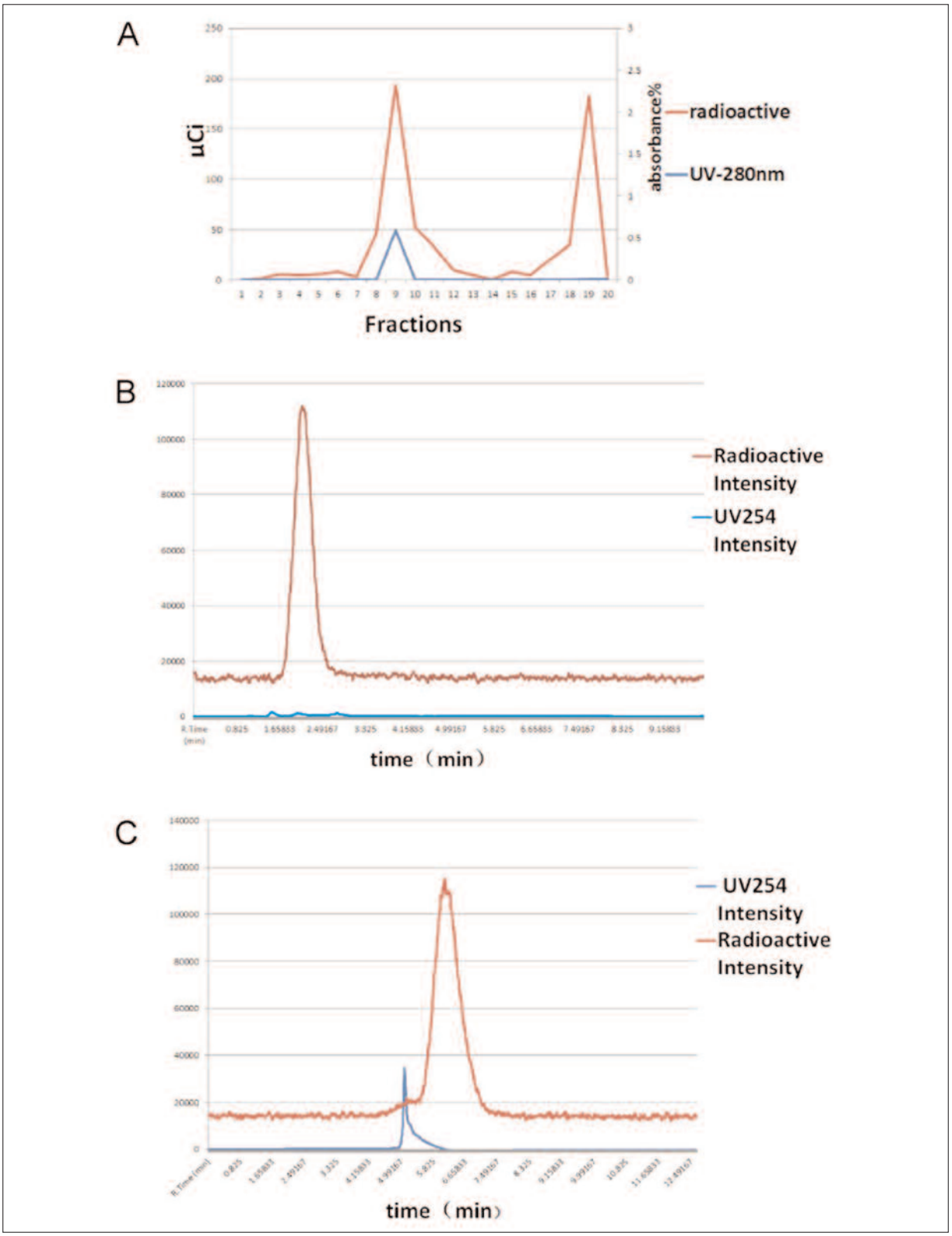

Figure 2. Chromatography analysis of ^{131}I-Hsp90α-mAb. Sephadex G-25 column was used. Elution rate: 0.5 ml/min, 5 drops/fraction. ***A,*** The radioactivity and the 280 nm UV absorbance results. ***B,*** HPLC analysis of pure free Na^{131}I. The radioactive retention time of pure free Na^{131}I is about 2.14 min. ***C,*** HPLC analysis of fraction 9 containing ^{131}I-Hsp90α-mAb. The retention time of ^{131}I-HSP90α-mAb is in about 5.13 min.

the analysis of eluted fractions. We see two radioactive peaks after chromatography. The first radioactive peak is at fraction 9 and the second at fraction 19 (Figure 2A). The first radioactive peak overlaps with the UV (280 nm) absorbance peak at fraction 9, indicating that this fraction contains ^{131}I-Hsp90α-mAb (Figure 2A). Furthermore, HPLC was employed to calculate the purity of the radiolabeled mAb. The pure free Na^{131}I was analyzed first and showed one single radioactive peak with the retention time in about 2.14 minutes (Figure 2B). Next, fraction 9 was analyzed by HPLC and showed one single UV254 absorbance peak at 5.13 min and one single radioactive peak at 6.24 min right after the UV absorbance peak. The results show that the retention time of ^{131}I-Hsp90α-mAb is in about 5.13 min. The results of HPLC analysis also revealed that the radiochemical purity of ^{131}I-Hsp90α-mAb was > 95.0%, which is adequate for using in both *in vitro* and *in vivo* experiments. In addition, we found that human blood serum does not affect the stability of ^{131}I-Hsp90α-mAb at 37°C (Figure 3A).

The Binding of ^{131}I-Hsp90α-mAb in the Cell is Specific

The cellular uptake of ^{131}I-Hsp90α-mAb was measured using DU145 cell culture in the presence or absence of unlabeled Hsp90α-mAb over the time course. As shown in Figure 3B, the

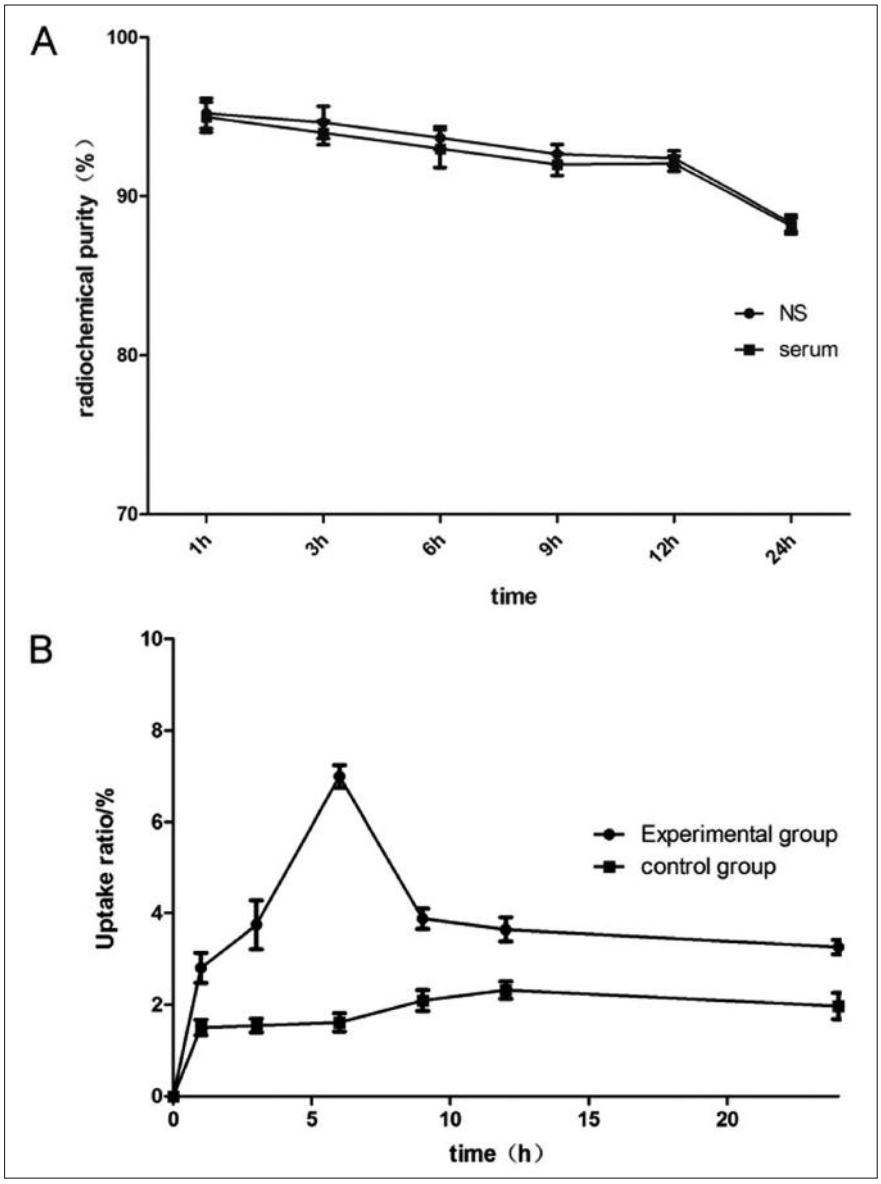

Figure 3. Stability of ^{131}I-Hsp90α-mAb and its cellular uptake. ***A,*** ^{131}I-Hsp90α-mAb was dissolved in saline or human blood serum and then incubated at 37°C for indicated time points. The radiochemical purity was then determined and presented graphically in percentage. ***B,*** DU145 cells were treated with or without unlabeled Hsp90α-mAb for half an hour and then incubated with ^{131}I-Hsp90α-mAb. The radioactivity of cellular uptake was then determined at the indicated time points and presented graphically in percentage.

presence of unlabeled Hsp90α-mAb in the control group significantly blocked the uptake of ^{131}I-Hsp90α-mAb, indicating that the cellular uptake of ^{131}I-Hsp90α-mAb is mainly resulted from the specific binding of ^{131}I-Hsp90α-mAb to Hsp90α.

Ability of ^{131}I-Hsp90α-mAb to Image Human Prostate Tumor in Mice Model

Figure 4A shows the SPECT imaging of mice bearing human prostate carcinoma at 3, 6, 9, and 12h post-injection of ^{131}I-Hsp90α-mAb. A high concentration of radioactivity was detected in the liver and spleen at 3 h post-injection in the presence of unlabeled Hsp90α-mAb in the control group. In contrast, a high concentration of radioactivity was accumulated in the tumor on the right armpit of the mouse in the absence of unlabeled Hsp90α-mAb in the experimental group. The results suggest that the unlabeled mAb significantly reduced the tumor uptake of ^{131}I-Hsp90α-mAb.

The maximum counts were recorded by drawing regions of interest (ROI) over the tumor and the homo-lateral muscle on the coronal images, respectively and then T/M ratio was calculated. T/M ratio in the experimental group was significantly higher than the block group (Figure 4B). ^{18}F-FDG micro-PET scan was performed to verify the *in vivo* phenotype of prostate cancer xenograft. As shown in the transverse, sagittal and coronal section, the presence of tumor was clearly seen (Figure 4C).

Discussion

The overexpression of Hsp90 has been shown to associate with the oncogenesis of prostate cancer. For example, elevated levels of Hsp90 were detected in the serum of patients with prostate cancer[18]. Hsp90 becomes a viable target in the treatment of prostate cancer[19-21]. High expression of Hsp90 represents an important oncogenic signaling node for malignant behavior in cancer. The detecting upregulation or activation of Hsp90 in cancer cells could serve as an early indicator of malignant behavior. Most of Hsp90 inhibitors selectively accumulate in tumors, but do not enter most of normal tissues[22], indicating that tumor Hsp90 proteins may behave differently from normal Hsp90. In addition, molecular imaging as a fascinating approach is being widely accepted in diagnostic nuclear imaging. The imaging probes based on antibody have been reported[23,24]. Therefore, study of radioactive mAb specific to Hsp90 will be required clinically for molecular imaging of a certain of tumors.

In this study, we reported the radiosynthesis and characteristics of ^{131}I-HSP90α-mAb and found that this new molecular probe preferentially adhered to prostate tumor. Our data are consistent with previous finding that Hsp90 is selectively accumulated in prostate tumor cells.

^{99m}Tc is the optimal radionuclide that is commonly used for SPECT imaging, but the labeling procedure requires $SnCl_2$. The disulfide bond in the Hsp90α-mAb may be destroyed in the presence of $SnCl_2$. Because this disulfide bond is essential for maintaining the stability of the Hsp90α-mAb, we chose ^{131}I instead of ^{99m}Tc to label Hsp90α-mAb. ^{131}I has a half-life of 8.02 days and emits not only α but also β rays, so that the ^{131}I-Hsp90α-mAb has an additive potential to be used as a reagent in tumor radioimmunotherapy.

In vivo scintigraphic imaging with ^{131}I-HSP90α-mAb revealed a higher tumor uptake in the mice bearing prostate tumor xenografts (Figure 4). However, radiotracer accumulation was also detected in the spleen and liver, which may indicate the limited application of ^{131}I-Hsp90α-mAb planar imaging in tumors in these organs.

Radioimmunotherapy has become an attractive therapeutic application due to its ability to target both the primary tumor site and disseminated diseased tissue[25,26]. Tumor cells absorb high amounts of energy in the form of photons or charged particles that could damage DNA strand[27] and induce not only apoptosis[28] but also programmed necrosis[29]. The observation that ^{131}I-Hsp90α-mAb can preferentially accumulate in the prostate tumor cell in this study prompts us to further study its application prospect in tumor radioimmunotherapy in the future research.

Conclusions

The Hsp90α-mAb can be successfully labeled with ^{131}I by Chloramine-T method. The radiochemical purity can reach 95% after purification. The labeled mAb is stable in human blood serum and can preferentially accumulate in the prostate

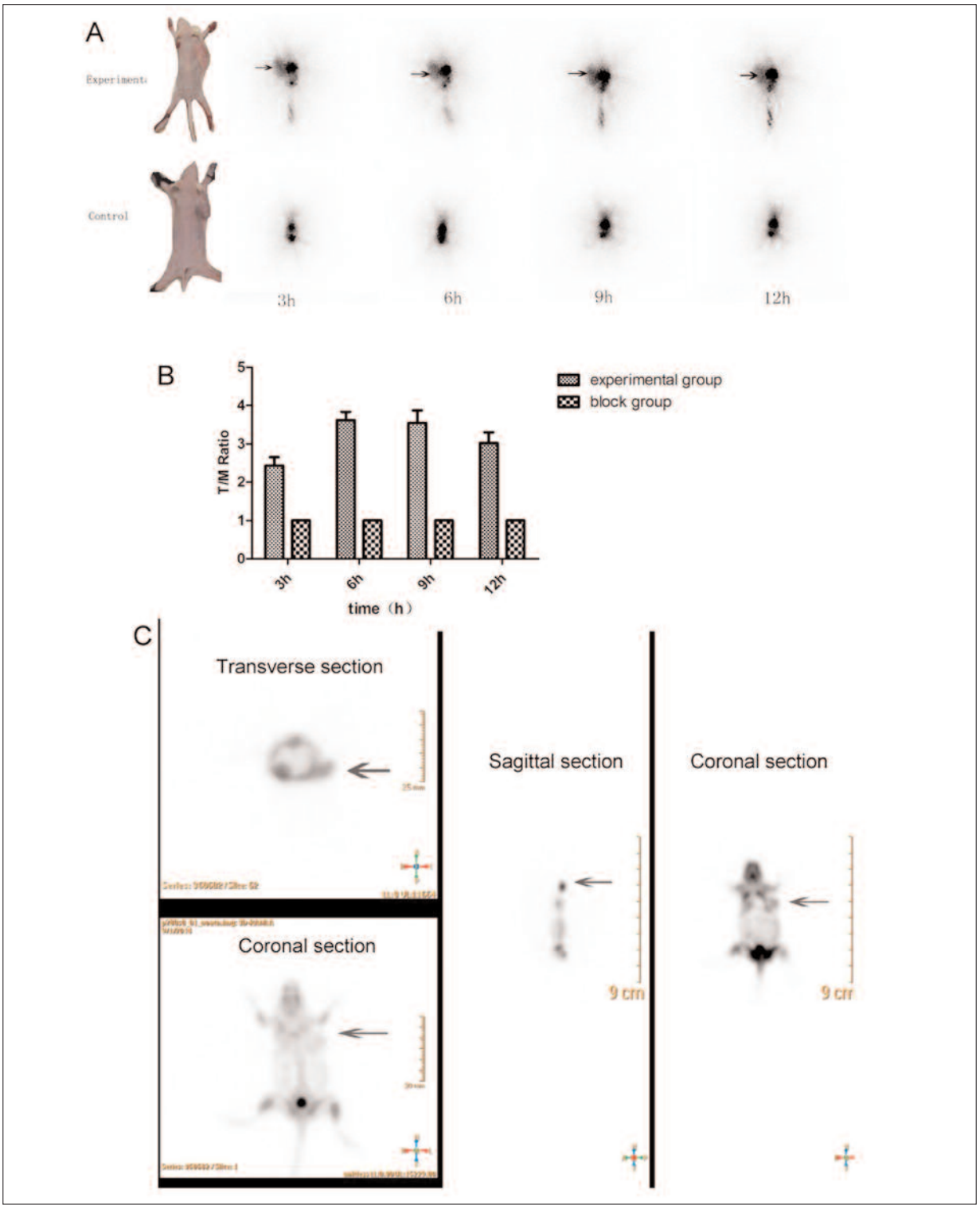

Figure 4. *In vivo* imaging. ***A,*** SPECT imaging. Mice bearing human prostate tumor xenograft were treated with saline (experimental group) or unlabeled Hsp90α-mAb (control group). After 1h, each animal was injected with ^{131}I-HSP90α-mAb. SPECT imaging was performed at the indicated time points. The visualized tumors are indicated with arrows. ***B,*** The maximum counts were recorded by drawing regions of interest (ROI) over the tumor and the homo-lateral muscle on the coronal images, respectively. T/M ratio was then calculated and graphically presented. ***C,*** ^{18}F-FDG micro-PET scan verified the *in vivo* phenotype of prostate tumor xenograft. As shown in the transverse, sagittal and coronal sections, the tumor was clearly seen. The average T/M ratio was 5.23. The arrow indicates the tumor.

tumor cell and successfully image the human prostate cancer xenograft. ^{131}I-Hsp90α-mAb is a promising molecular probe for detecting prostate tumors.

Acknowledgements

This study was supported by grants from the National Natural Science Foundation of China (NSFC 81071183), National Major Scientific Equipment Special Fund (2011YQ03011409), and Key Projects in the National Science & Technology Pillar Program during the Twelve Five-year Plan Period (2014BAA03B03).

Conflict of Interest

The Authors declare that there are no conflicts of interest.

References

1) Burrows F, Zhang H, Kamal A. Hsp90 activation and cell cycle regulation. Cell Cycle 2004; 3: 1530-1536.
2) Johnson JL. Evolution and function of diverse Hsp90 homologs and cochaperone proteins. Biochim Biophys Acta 2011; 1823: 607-613.
3) Jackson SE. Hsp90: structure and function. Top Curr Chem 2012; 328: 155-240.
4) Taipale M, Taipale M, Krykbaeva I, Koeva M, Kayatekin C, Westover KD, Karras GI, Lindquist S. Quantitative analysis of HSP90-client interactions reveals principles of substrate recognition. Cell 2012; 150: 987-1001.
5) Kundrat L, Regan L. Balance between folding and degradation for Hsp90-dependent client proteins: a key role for CHIP. Biochemistry 2010; 49: 7428-7438.
6) Snigireva AV, Vrublevskaya VV, Skarga YY, Evdokimovskaya YV, Morenkov OS. Effect of heat shock protein 90 (Hsp90) on migration and invasion of human cancer cells *in vitro*. Bull Exp Biol Med 2014; 157: 476-478.
7) Liu XG, Guo Y, Yan ZQ, Guo MY, Zhang ZG, Guo CA. FAK/c-Src signaling pathway mediates the expression of cell surface HSP90 in cultured human prostate cancer cells and its association with their invasive capability. Zhonghua Zhong Liu Za Zhi 2011; 33: 340-344.
8) Khattar V, Fried J, Xu B, Thottassery JV. Cks1 proteasomal degradation is induced by inhibiting Hsp90-mediated chaperoning in cancer cells. Cancer Chemother Pharmacol 2015; 75: 411-420.
9) Sreedhar AS, Kalmar E, Csermely P, Shen YF. Hsp90 isoforms: functions, expression and clinical importance. FEBS Lett 2004; 562: 11-15.
10) Wandinger SK, Richter K, Buchner J. The Hsp90 chaperone machinery. J Biol Chem 2008; 283: 18473-18477.
11) Gong AJ, Gong LL, Yao WC, Ge N, Lu LX, Liang H. Aplysin induces apoptosis in glioma cells through HSP90/AKT pathway. Exp Biol Med (Maywood) 2014; Epub ahead of print.
12) Bertelsen V, Stang E. The Mysterious Ways of ErbB2/HER2 Trafficking. Membranes (Basel) 2014; 4: 424-446.
13) Lee SH, Jee JG, Bae JS, Liu KH, Lee YM. A group of novel HIF-1alpha inhibitors, glyceollins, blocks HIF-1alpha synthesis and decreases its stability via inhibition of the PI3K/AKT/mTOR pathway and Hsp90 Binding. J Cell Physiol 2014; 230: 853-862.
14) Bellotti C, Castagnola G, Tierno SM, Centanini F, Sparagna A, Vetrone I, Mezzetti G. Radioguided surgery with combined use of gamma probe and hand-held gamma camera for treatment of papillary thyroid cancer locoregional recurrences: a preliminary study. Eur Rev Med Pharmacol Sci 2013; 17: 3362-3366.
15) Menendez Torre E, Lopez Carballo MT, Rodriguez Erdozain RM, Forga Llenas L, Goni Iriarte MJ, Barberia Layana JJ. Prognostic value of thyroglobulin serum levels and ^{131}I whole-body scan after initial treatment of low-risk differentiated thyroid cancer. Thyroid 2004; 14: 301-306.
16) Wang W, Macapinlac H, Larson SM, Yeh SD, Akhurst T, Finn RD, Rosai J, Robbins RJ. [18F]-2-fluoro-2-deoxy-D-glucose positron emission tomography localizes residual thyroid cancer in patients with negative diagnostic (131)I whole body scans and elevated serum thyroglobulin levels. J Clin Endocrinol Metab 1999; 84: 2291-2302.
17) Zakani A, Saghari M, Eftekhari M, Fard-Esfahani A, Fallahi B, Esmaili J, Assadi M. Evaluation of radioiodine therapy in differentiated thyroid cancer subjects with elevated serum thyroglobulin and negative whole body scan using 131I with emphasize on the thallium scintigraphy in these subgroups. Eur Rev Med Pharmacol Sci 2011; 15: 1215-1221.
18) Burgess EF, Ham AJ, Tabb DL, Billheimer D, Roth BJ, Chang SS, Cookson MS, Hinton TJ, Cheek KL, Hill S, Pietenpol JA. Prostate cancer serum biomarker discovery through proteomic analysis of alpha-2 macroglobulin protein complexes. Proteomics Clin Appl 2008; 2: 1223.
19) Centenera MM, Fitzpatrick AK, Tilley WD, Butler LM. Hsp90: still a viable target in prostate cancer. Biochim Biophys Acta 2013; 1835: 211-218.
20) Albany C, Hahn NM. Heat shock and other apoptosis-related proteins as therapeutic targets in prostate cancer. Asian J Androl 2014; 16: 359-363.
21) Hance MW, Dole K, Gopal U, Bohonowych JE, Jezierska-Drutel A, Neumann CA, Liu H, Garraway IP, Isaacs JS. Secreted Hsp90 is a novel regulator of the epithelial to mesenchymal transition (EMT) in prostate cancer. J Biol Chem 2012; 287: 37732-37744.

22) Chiosis G, Neckers L. Tumor selectivity of Hsp90 inhibitors: the explanation remains elusive. ACS Chem Biol 2006; 1: 279-284.

23) Pysz MA, Gambhir SS, Willmann JK. Molecular imaging: current status and emerging strategies. Clin Radiol 2010; 65: 500-516.

24) Duatti A. Molecular imaging with endogenous and exogenous ligands: The instance of antibodies, peptides, iodide and cupric ions. Nucl Med Biol 2014; Epub ahead of print.

25) Kawashima H. Radioimmunotherapy: a specific treatment protocol for cancer by cytotoxic radioisotopes conjugated to antibodies. Scientific World Journal 2014; 2014: 492061.

26) Prise KM, O'Sullivan JM. Radiation-induced bystander signalling in cancer therapy. Nat Rev Cancer 2009; 9: 351-360.

27) Bertout JA, Patel SA, Simon MC. The impact of O_2 availability on human cancer. Nat Rev Cancer 2008; 8: 967-975.

28) Kroemer G, Galluzzi L, Brenner C. Mitochondrial membrane permeabilization in cell death. Physiol Rev 2007; 87: 99-163.

29) Cabon L, Galan-Malo P, Bouharrour A, Delavallee L, Brunelle-Navas MN, Lorenzo HK, Gross A, Susin SA. BID regulates AIF-mediated caspase-independent necroptosis by promoting BAX activation. Cell Death Differ 2011; 19: 245-256.